Research Article **Open Access**

Christina Körbel*, Maximilian Linxweiler, Florian Bochen, Silke Wemmert, Bernhard Schick, Markus Meyer, Hans Maurer, Michael D Menger, Richard Zimmermann, Markus Greiner

Treatment of *SEC62* over-expressing tumors by Thapsigargin and Trifluoperazine

https://doi.org/10.1515/bmc-2018-0006
received January 25, 2018; accepted March 16, 2018.

Abstract: Treatment with analogues of the SERCA-inhibitor Thapsigargin is a promising new approach for a wide variety of cancer entities. However, our previous studies on various tumor cells suggested resistance of *SEC62* over-expressing tumors to this treatment. Therefore, we proposed the novel concept that e.g. lung-, prostate-, and thyroid-cancer patients should be tested for *SEC62* over-expression, and developed a novel therapeutic strategy for a combinatorial treatment of *SEC62* over-expressing tumors. The latter was based on the observations that treatment of *SEC62* over-expressing tumor cells with *SEC62*-targeting siRNAs showed less resistance to Thapsigargin as well as a reduction in migratory potential and that the siRNA effects can be mimicked by the Calmodulin antagonist Trifluoperazine. Therefore, the combinatorial treatment of *SEC62* over-expressing tumors was proposed to involve Thapsigargin and Trifluoperazine. Here, we addressed the impact of Thapsigargin and Trifluoperazine in separate and combined treatments of heterotopic tumors, induced by inoculation of human hypopharyngeal squamous cell carcinoma (FaDu)-cells into the mouse flank. Seeding of the tumor cells and/or their growth rate were significantly reduced by all three treatments, suggesting Trifluoperazine is a small molecule to be considered for future therapeutic strategies for patients, suffering from Sec62-overproducing tumors.

Keywords: Calmodulin antagonists; endoplasmic reticulum; Sec62 protein; Trifluoperazine; tumor therapy.

Introduction

Differentiation of cancer patients with respect to molecular markers is cutting edge in the field of cancer therapeutics. Many genetic alterations are known for non-small cell lung cancer and this may allow for a more personalized treatment (1). On a molecular level, a personalized approach is often based on the fact that some patients do not respond to therapeutics due to specific resistance mechanisms. One promising new approach for the treatment of a wide spectrum of cancer entities is the use of a Thapsigargin-analogue named Mipsagargin (2, 3). Thapsigargin itself is an irreversible blocker of the Sarco-/Endoplasmic Reticulum Calcium ATPase (SERCA) and prevents the reuptake of calcium from the cytosol to the Endoplasmic Reticulum (ER) (4). This leads to an increase in cytosolic calcium concentration and subsequently to apoptotic cell death (5). Over the last 15 years, a variety of Thapsigargin-analogues were synthesized to overcome the systemic toxicity of Thapsigargin and for targeted therapy (5-8). By adding a synthetic peptide, cell entry through the plasma membrane of these analogues is prevented therefore only targeted cells which present the Prostate Specific Membrane Antigen (PSMA) on their surface or producing Prostate Specific Antigen (PSA), which cleaves the peptide thereby producing free Thapsigargin (9-11). Thus, this therapeutic approach works on a broad spectrum of tumors expressing PSMA on the tumor cell surface or on the surface of tumor neovasculature epithelial cells (12). However, the success of such a treatment strongly depends on the sensitivity of the attacked cells towards Thapsigargin which, following our previously published results, depends on the Sec62

***Corresponding author: Christina Körbel,** Institute for Clinical and Experimental Surgery, Saarland University, Homburg/Saar, Germany, E-mail: Christina.Koerbel@uks.eu
Michael D Menger: Institute for Clinical and Experimental Surgery, Saarland University, Homburg/Saar, Germany
Maximilian Linxweiler, Florian Bochen, Silke Wemmert, Bernhard Schick: Department of Otorhinolaryngology, Head and Neck Surgery, Saarland University Hospital, Homburg/Saar, Germany
Markus Meyer, Hans Maurer: Department of Experimental and Clinical Toxicology, Saarland University, Homburg/Saar, Germany
Richard Zimmermann, Markus Greiner: Department of Medical Biochemistry and Molecular Biology, Saarland University, Homburg/Saar, Germany

content of the respective cells (13). Sec62 is a membrane protein of the ER located at the polypeptide-conducting channel in the ER membrane, the Sec61-complex, and interacts with Sec61α and Sec63 (14, 15). In mammalian cells Sec62 can also interact with the ribosomal tunnel exit, thereby supporting co-translational protein import into the ER (16). The Sec61 channel not only acts as a protein conducting pore but also as an important calcium leak channel, which is regulated by Calmodulin interaction on the cytosolic surface (17-19) and by BiP interaction on the ER luminal surface (20). Therefore, Sec62 not only supports protein translocation but is also involved in the regulation of ER calcium homeostasis (13, 19). In our previous studies, we demonstrated a siRNA mediated Sec62 depletion leads to an increase in cytosolic calcium concentration and an increased Sec62 protein content on the one hand protects tumor cells from Thapsigargin induced cell death and on the other hand siRNA mediated depletion of Sec62 sensitizes the tumor cells for Thapsigargin treatment (13). Furthermore, Sec62 directly interacts with Sec61α close to its Calmodulin interacting IQ-motif in a calcium sensitive manner (19). An over-expression of a *SEC62D308A* mutant, lacking a computationally predicted EF-hand calcium binding motif, in HEK293 cells also led to an increased cytosolic calcium concentration, in the same way as we observed before for Sec62 depletion (19). This supports a model in which Sec62 detects calcium ions leaking from the ER through the Sec61 channel by a conformational change allowing the Calmodulin binding to Sec61α which subsequently closes the channel. Following this model, the Sec62 depletion or over-expression of *SEC62D308A* handicaps Calmodulin binding to the Sec61α thus explaining the increased calcium leakage. Most interestingly, the same system could also be attacked from the other side, the addition of the Calmodulin antagonists Trifluoperazine or Ophiobolin A perfectly mimicked the Sec62 depletion phenotype with respect to calcium leakage and sensitized tumor cells for Thapsigargin (21). This paved the way for proposing a new therapeutic option to treat patients with Sec62-overproducing tumors by using a combination therapy of Calmodulin antagonists to sensitize the cells for calcium stress followed by Thapsigargin to induce cell death. Since we previously observed Sec62-overproduction as a common phenomenon in cancers of the prostate, lung and thyroid (22, 23), this new approach would broaden the use of targeted Thapsigargin therapy and increase its efficiency, especially for patients with more aggressive tumors. For example, in prostate cancer where Sec62-overproduction correlates with increasing de-differentiation as well as a higher invasiveness of tumor cells (22) and in lung cancer patients suffering from tumors with a high Sec62 content have a bad prognosis (23).

In this study we evaluated the toxicity of the proposed combined therapy and provided evidence of its effectiveness using Thapsigargin and Trifluoperazine treatment alone or in combination on tumor cell growth, employing a heterotopic mouse flank tumor model of Sec62-overproducing human FaDu hypopharyngeal squamous cell carcinoma.

Methods

Human cell culture

To prepare the tumor cells, UM-SCC1 and FaDu cells were cultured in DMEM (Gibco Invitrogen, Karlsruhe, Germany) containing 10% fetal bovine serum (FBS; Biochrom, Berlin, Germany) and 1% penicillin/streptomycin (PAA Laboratories GmbH, Pasching, Austria), LnCap cells were cultured in RPMI (PAA Laboratories GmbH) containing the same supplements in a humidified environment with 5% CO_2 at 37°C. The cells were thawed, cultured for three passages, then harvested, counted and the required cell number was adjusted in 100 µl PBS (Gibco Invitrogen). For cytogenetic analysis, metaphase cells were fixed with methanol/acetic acid (3:1) and banded with Giemsa trypsin.

Fluorescence- in situ- hybridization (FISH)

FISH analysis was performed on unstained cytogenetic preparations pre-treated with RNase A and pepsin (Sigma-Aldrich, Munich, Germany), post-fixation with 4% paraformaldehyde/PBS, subsequent dehydration in an ethanol series and followed by air-drying. DNA from Bacterial artificial chromosome clone (BAC) (SEC62; (RP11-379K17) purchased from ImaGenes (Berlin, Germany) was extracted using the NucleoBond®PC100 Kit (Macherey-Nagel, Dueren, Germany) and labelled with biotin using the BioPrime DNA Labeling System (Invitrogen, Life Technologies, Darmstadt, Germany) according to the manufacturers' instructions. Hybridization was performed in 50% formamide/2× SSC and COT-1 DNA (Roche Diagnostics, Mannheim, Germany) overnight in a moist chamber at 37°C. Post-hybridization washing were performed three times in 50% formamide/2× SSC at 42°C and two times in 2× SSC at 42°C. Fluorescence detection

of the biotin signals was performed using fluorescein-isothiocyanate (Vector Laboratories, Burlingame, CA), and the nuclei were counterstained with a DAPI anti-fade solution (Vector Laboratories). Images were acquired using an Olympus BX61 microscope (Olympus, Hamburg, Germany) and documented with ISIS digital image analysis software system (Metasystems, Altlussheim, Germany).

Comparative genomic hybridization (CGH)

CGH was performed as described previously (24). Briefly, genomic DNA from FaDu cell line and reference DNA from blood of a healthy donor were obtained using standard phenol/chloroform extraction, labeled with biotin and digoxigenin by nick translation according to the manufacturer's protocol (Roche Diagnostics). Hybridization was performed together with COT-1 DNA (Roche Diagnostics) to normal chromosome metaphase spreads from peripheral blood lymphocytes prepared using standard procedures. Post-hybridization washes were performed with 50% formamide/2× standard saline citrate (SSC), 2× SSC and 0.1× SSC at 45°C. DNA was visualized with fluorescein-isothiocyanate (Vector Laboratories) and rhodamine (Roche Diagnostics), respectively, and counterstained with a DAPI (4, 6-diamidino-2-phenylindole) anti-fade solution (Vector Laboratories). Fluorescence images were captured using an Olympus BX61 microscope (Olympus) and image processing was performed using the ISIS digital image analysis software system (Metasystems). Average ratio profiles were determined from the analysis of 12-15 metaphases. The heterochromatic regions in chromosomes 1, 9 and 16, the p-arms of the acrocentric chromosomes, and Y chromosome were excluded from the analysis because of suppression of hybridization with Cot-1 DNA in these regions.

Animals

For the study, eight-week-old female athymic nude mice (BALB/cAnNRj-Foxn1nu/Foxn1nu; Janvier Lab, Le Genest-Saint-Isle, France) with a body weight of about 24 g were used. The mice were housed in groups of five mice in isolated ventilated cages under specific pathogen-free conditions in a temperature- and humidity-controlled 12-hour light/dark environment in the animal facility of the Institute for Clinical and Experimental Surgery (Saarland University, Germany) and had free access to tap water and standard pellet food. All animal experiments were performed in accordance with the German legislation on protection of animals, the EU Directive 2010/63/EU and the National Institutes of Health Guidelines for the Care and Use of Laboratory Animals (NIH Publication #85-23 Rev. 1985) and were approved by the local governmental animal care committee.

Subcutaneous tumor model

For subcutaneous tumor cell inoculation, mice were anesthetized with 2% isoflurane in oxygen and fixed in prone position. In a pretrial UM-SCC1, FaDu and LnCap cells were injected subcutaneous into both flanks of four mice per group. Whereby, 100 µl of a tumor cell suspension with 1×10^6 tumor cells were injected into the left flank and 5×10^6 tumor cells were injected into the right flank of each mouse. Then we injected 100 µl of a 1×10^6 FaDu cell suspension into each flank of 24 eight-week-old mice. Afterwards further animals were injected with 100 µl of a 2.5×10^5 FaDu cell suspension into each flank of 40 eight-week-old mice. After removing the needle, the inoculation channel was then recapped with micro-forceps to avoid recoil of the tumor cell suspension and to ensure a spheroid tumor growth. To monitor subcutaneous tumor growth, caliper measurments were taken at least once per week. The tumor volume was calculated using the standard ellipsoid formula, $V = /6 \times L \times W^2$ (where L is the longest diameter and W is the perpendicular smaller diameter (25)).

Treatment of mice

In the first treatment study, 24 tumor bearing athymic mice were randomly divided into two groups and treated over three weeks, three times a week in 48 h or 72 h intervals. Treatments were as follows, an intraperitoneal (i.p.) and/or intravenous (i.v) injection of either vehicle (n=12) or a combination of 0.5 mg/kg i.p. Trifluoperazine and 0.8 mg/kg i.v. Thapsigargin (10) (n=12).

Before treating tumor bearing mice with i.p. Thapsigargin, the absorption of the substances was analyzed. Initially, five mice were injected with 1.6 mg/kg Thapsigargin either via i.v. (n=3) or i.p (n=2). To determine the concentration of Thapsigargin, we sampled blood after 6 , 24 and 48 hours and immediately analyzed serum by mass spectrometry. Afterwards, 1.6 mg/kg Thapsigargin and 0.5 mg/kg Trifluoperazine were i.p. injected at an interval of 1 h to guarantee absorption without risk of

compound interaction in the abdominal cavity. The blood samples were analyzed after 48 h and 168 h by mass spectrometry.

Furthermore, 40 tumor bearing athymic mice were randomly divided into four groups and treated over five weeks, three times a week in 48 h or 72 h intervals by i.p. injection of either vehicle (n=10), 0.5 mg/kg Trifluoperazine (n=10), 1.6 mg/kg Thapsigargin (n=10) or the combination of both substances (n=10). An interval of 1 h between the two injections was given to ensure valid absorption. Moreover, the mice were monitored at least once a week, scoring appearance, behavior, food and water intake, respiration rate, and body weight to evaluate burden. At the end of the *in vivo* experiments, mice were sacrificed using an overdose of anesthetics and tumors were carefully excised and further processed for immunohistochemical analyses.

Ultrasound imaging

At the end of the observation period, the tumors were also analyzed using a high-resolution ultrasound system. Mice were anesthetized using 4% isoflurane in oxygen and fixed in prone position on a heated platform. Anesthesia was further maintained with 2% isoflurane. Ultrasound coupling gel (Aquasonic 100, Parker Laboratories Inc., Fairfield, N.J., USA) was applied to the dorsal skin, and ultrasound imaging was performed using the Vevo 770 high-resolution ultrasound system (VisualSonics, Toronto, Canada) by means of real-time microvisualization 707B scanhead with a center frequency of 30 MHz and a focal depth of 13 mm. An automated computer-controlled stepping motor moved the 30-MHz ultrasound scanhead over the mouse's skin, acquiring two-dimensional images at parallel and uniformly spaced 100-µm intervals. The predefined parallel geometry of the two-dimensional images allowed fast three-dimensional image reconstruction. Tumors were identified on the three-dimensional ultrasound images and measured in the treatment groups consecutively.

Immunohistochemistry

Formalin-fixed specimens of subcutaneous tumors at day 35 were embedded in paraffin. A Leica RM 2265 rotary microtome (Leica Microsystems, Wetzlar, Germany) was used to cut 2 µm thick sections for immunohistochemical staining of Sec62 and Ki67. Upon deparaffinization, heat-induced epitope retrieval was performed for 15 minutes by incubation in TRIS-EDTA-buffer (pH 9.0) at 95°C for the staining of Ki67. Unspecific protein binding sites were blocked with 3% goat-serum (Dianova, Hamburg, Germany) in PBS for 30 minutes at room temperature. Subsequently, primary antibody incubation was performed overnight at 4°C. Proliferating cells were stained with a primary polyclonal rabbit antibody directed against the antigen region of human Ki67 (1:500; Abcam, Cambridge, UK). Tissue sections were then incubated using a biotinylated secondary goat anti-rabbit IgG antibody (ready-to-use; Abcam) and a streptavidin-peroxidase conjungate (ready-to-use; Abcam). As chromogen 3,3′-diaminobenzidine tetrahydrochloride was used, slides were counterstained with 1% Mayers Hemalaun solution (Merck, Darmstadt, Germany).

For Sec62 staining, heat-induced epitope retrieval was performed for 30 minutes by incubation in 10 mM citrate buffer (pH 6.0) at 95°C. Unspecific protein binding sites were blocked with 3% BSA (Sigma-Aldrich) in PBS for 30 minutes at room temperature. Primary antibody incubation was performed for 1 h at room temperature, using an affinity-purified polyclonal rabbit anti-peptide antibody directed against the C terminus of human Sec62 (1:400; self-made). Visualization was performed using the REAL detection system Alkaline Phosphatase (Agilent Technologies, Waldbronn, Germany), according to the manufacturer's instructions; the slides were counterstained with hematoxylin (Sigma-Aldrich).

For each group, sections from 6 randomly chosen animals (one section per tumor) were analyzed by light microscopy using an Olympus BX60 microscope. Central necrosis (given as a % of the tumor section) was assessed by dividing the necrotic area by the whole tumor area of the section and multiplied by 100. The fraction of proliferating cells (given as % of all analyzed cells) was calculated by dividing the number of Ki67-positive cells in a tumor section by the overall number of cells in this section multiplied by 100. To analyze non-uniform staining intensities in tumors, the Sec62-immunoreactivity was evaluated using a modified version of the immunoreactive score (IRS). The IRS rates the staining intensity from zero to three and the percentage of the stained cells from zero to four (<10%, 10-50%, 51-80%, >80%)(26). The two major staining intensities of the specimen were identified and rated according to the conventional IRS (score ranging from 0 to 12). Thereby the total percentage of evaluated cells must not exceed 100%. The sum of these two single scores resulted in the modified IRS (mIRS; score ranging from 0 to 14).

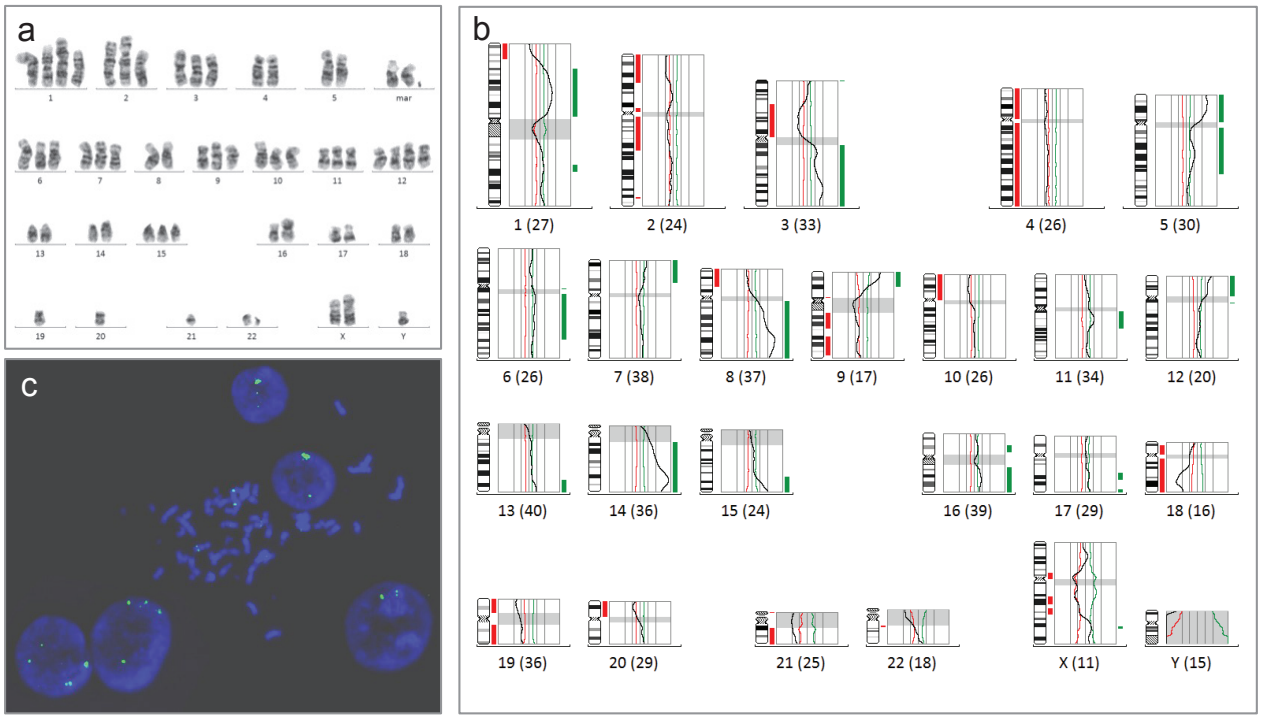

Figure 1: Genetic alterations in FaDu cell line. **a:** Karyotype analysis by GTG-banding indicated a highly complex karyotype with numerous marker chromosomes and numerous translocation chromosomes in FaDu metaphase spreads. **b:** CGH profile of FaDu cell line shows high-level amplifications of 3q25.3q27, 8q22q24.2 and 14q24.3qter, gains of 1p13.1p33, 1q25.3, 3q, 5p, 5q11.2q31.1, 6q12q24, 7p14pter, 8q, 9p21pter, 11q11.1q14.1, 12p, 13q32qter, 14, 15q24qter, 16p11.1, 16q, 17q21.3q22, and 17q25, and losses of 1p35pter, 2p11.2, 2p21pter, 2q11.2q22, 3p11.1p21.3, 4, 8p21.2pter, 9q13q21.3, 9q32q34.3, 10p, 18p11.2, 18q, 19, 20p and 21. Bars to the left (red) and right (green) of each chromosome indicate losses and gains, respectively. The numbers in brackets represent the number of metaphase chromosomes investigated for analysis shown in the profile. **c:** FISH analysis of interphase nuclei and metaphase spread with a *SEC62*-specific BAC probe (green). The insert shows nuclei with two and four *SEC62* signals, respectively, together with an amplification of *SEC62* (green: *SEC62*, blue: DAPI counterstain, magnification 60x).

Statistics

After testing the data for normal distribution and equal variance, differences between two experimental groups were assessed using an unpaired Student's t-test. Differences between multiple groups were analyzed by ANOVA followed by the Duncan's Multiple Range test with correction of the alpha error according to Bonferroni probabilities to compensate for multiple comparisons (SimaPlot 11.0; Jandel Corporation, San Rafael, CA, USA). All values were expressed as means ± SEM. Statistical significance was accepted when the p-value was less than 0.05.

Results

In a first approach karyotype analysis of the cell lines UM-SCC1 (data not shown) and FaDu using GTG-banding or CGH had indicated a highly complex karyotype with numerous marker chromosomes and numerous translocations (Figure 1a). CGH analysis showed DNA copy number gains in the 1p13.1p33, 1q25.3, 3q, 5p, 5q11.2q31.1, 6q12q24, 7p14pter, 8q, 9p21pter, 11q11.1q14.1, 12p, 13q32qter, 14, 15q24qter, 16p11.1, 16q, 17q21.3q22, and 17q25 region. High-level amplifications were observed on 3q25.3q27, 8q22q24.2 and 14q24.3qter. Significant copy number losses were detected in the 1p35pter, 2p11.2, 2p21pter, 2q11.2q22, 3p11.1p21.3, 4, 8p21.2pter, 9q13q21.3, 9q32q34.3, 10p, 18p11.2, 18q, 19, 20p and 21 regions. This CGH profile is represented in Figure 1b. Additional FISH analysis confirmed that FaDu cells exhibit increased copy numbers (amplification) of *SEC62* located in the 3q26.3 region as indicated by CGH (Figure 1c).

A mouse study was used to compare the growth of Sec62-overproducing UM-SCC1 or FaDu head and neck squamous cell carcinoma cells with the non-overproducing LnCap prostate cancer cells using a heterotopic athymic nude mouse model (n=12). While there was no tumor growth at all in four mice when we injected 1×10^6 (left)

or 5× 10^6 (right) LnCap cells to the flank of eight-week-old athymic mice, the four mice injected with UM-SCC1 cells in all cases led to tumor growth. Tumor volumes were very heterogeneous, both ultrasound and macroscopic examination revealed many intratumoral cysts, which hindered a reliable calculation of tumor volume by caliper (Figure 2a-d). This was the opposite for FaDu cells. Here we injected the same cell numbers to the flank of four individual mice and observed equal growth on either side with none or very few cysts (Figure 2e-h). Using 1× 10^6 cells, tumor volume reached 581 mm^3 after 28 days, with 5× 10^6 cells reaching 1572 mm^3 (Figure 2h). Therefore, we decided to use FaDu cells for all further investigations.

In the first treatment study, we analyzed the tumor growth of mice treated with a combination of Thapsigargin and Trifluoperazine and compared these to untreated animals. Here 1× 10^6 FaDu cells were injected into each flank of 24 eight-week-old athymic nude mice on day 0. We divided the animals into two groups and treated them either with a solvent control (n=12) or the combination of 0.5 mg/kg i.p.Trifluoperazine and 0.8 mg/kg i.v. Thapsigargin (10) (n=12). Treatment was performed from day 0 over an observation period of 20 days, three times a week in 48 h or 72 h intervals. We measured the tumor size at least once a week by caliper. The treatment group showed a minor reduction in tumor growth during the 20 days of observation compared to the control group (Figure 2i). The mice did not show any differences in weight gain between the two groups (Figure 2j).

Next, we determined the concentrations of Thapsigargin and Trifluoperazine which could be used for the treatment of the mice without toxic effect. This study of absorption level was necessary as literature for Thapsigargin was limited to the Thapsigargin-analogue L12-ADT only and used BALB/c-mice, which did not tolerate a single application of more than 0.8 mg/kg i.v. L12-ADT (10). For Trifluoperazine alone, a non-toxic dose of 0.5 mg/kg i.p. was published (27) but there was no data available for the combined use of Thapsigargin and Trifluoperazine. Firstly, we compared 1.6 mg/kg i.v. Thapsigargin (n=3) versus 1.6 mg/kg i.p. Thapsigargin (n=2) in athymic nude mice. We analyzed serum concentrations of Thapsigargin after 6 h, 24 h and 48 h by mass spectrometry. All animals behaved normally within these 48 h, but the analysis revealed high peak concentrations of Thapsigargin in at least one animal from the i.v. injected group, increasing the risk of toxic effects. The i.p. application led to more evenly distributed serum concentrations and therefore we decided to use this form of administration for further analysis (data not shown). Next, we determined the absorption rate of the combined therapy in three athymic nude mice, treating them on day 0, 2, 4 and 7 after tumor cell injection with 1.6 mg/kg Thapsigargin and 0.5 mg/kg Trifluoperazine (both i.p.), with 1 h left between injections to limit substance interactions. We analyzed the serum concentration of both substances on day 2 and 7 and monitored the animals for signs of toxicity. The analysis of serum concentrations showed an equal distribution in all animals for Thapsigargin and Trifluoperazine as well as a slight accumulation of the substances over the time period of 7 days (Figure 3). All animals showed normal grooming and movement behavior, food and water intake did not differ in-between the groups and accelerated respiration rate was not observed, suggesting repeated treatment with 1.6 mg/kg i.p. Thapsigargin and 0.5 mg/kg i.p. Trifluoperazine was non-toxic and therefore optimal for further studies.

Finally, we used the optimized treatment conditions to examine the impact of either Thapsigargin or Trifluoperazine treatment on tumor cell growth in the above mentioned heterotopic mouse flank model alone or in combination and compared this to tumor cell growth in untreated animals. Here 2.5× 10^5 FaDu cells were injected in each flank of 40 eight-week-old athymic nude mice. We divided the animals into four groups and administered an i.p. solvent control (n=10), 0.5 mg/kg Trifluoperazine (n=10), 1.6 mg/kg Thapsigargin (n=9, one animal died during the first observation week) or the combined therapy with both substances (n=10). Treatment was performed from day 0 over five weeks, three times a week in 48 h or 72 h intervals. We measured the tumor size at least once a week by caliper. All treatments resulted in a reduced number of macroscopic detectable tumors compared to the solvent control (Figure 4a). Thus 75% of the tumor cells injected led to tumor seeding in the control group, this was reduced to 40% by Trifluoperazine treatment and 28% by Thapsigargin treatment at day 14. The combined treatment with both substances led to tumor growth in 25%, up to day 28 (Figure 4b). Accordingly, the repetitive analyses of the detectable tumors exhibited a markedly slower tumor growth in the treatment groups compared to the control group (Figure 4c). Treatment with Trifluoperazine alone led to a faster increase in tumor size when compared to Thapsigargin alone. Up to day 21, there was no difference between the combined therapy and Thapsigargin alone, but from day 21 to day 35, tumor growth in the Thapsigargin group was slightly reduced (Figure 4c). Moreover, ultrasound analyses confirmed that the tumor volume of Thapsigargin treated mice and mice treated with both substances were significantly smaller than the tumor volume of control animals at day 35 (Figure 4d, f-i). During the whole observation time all animals

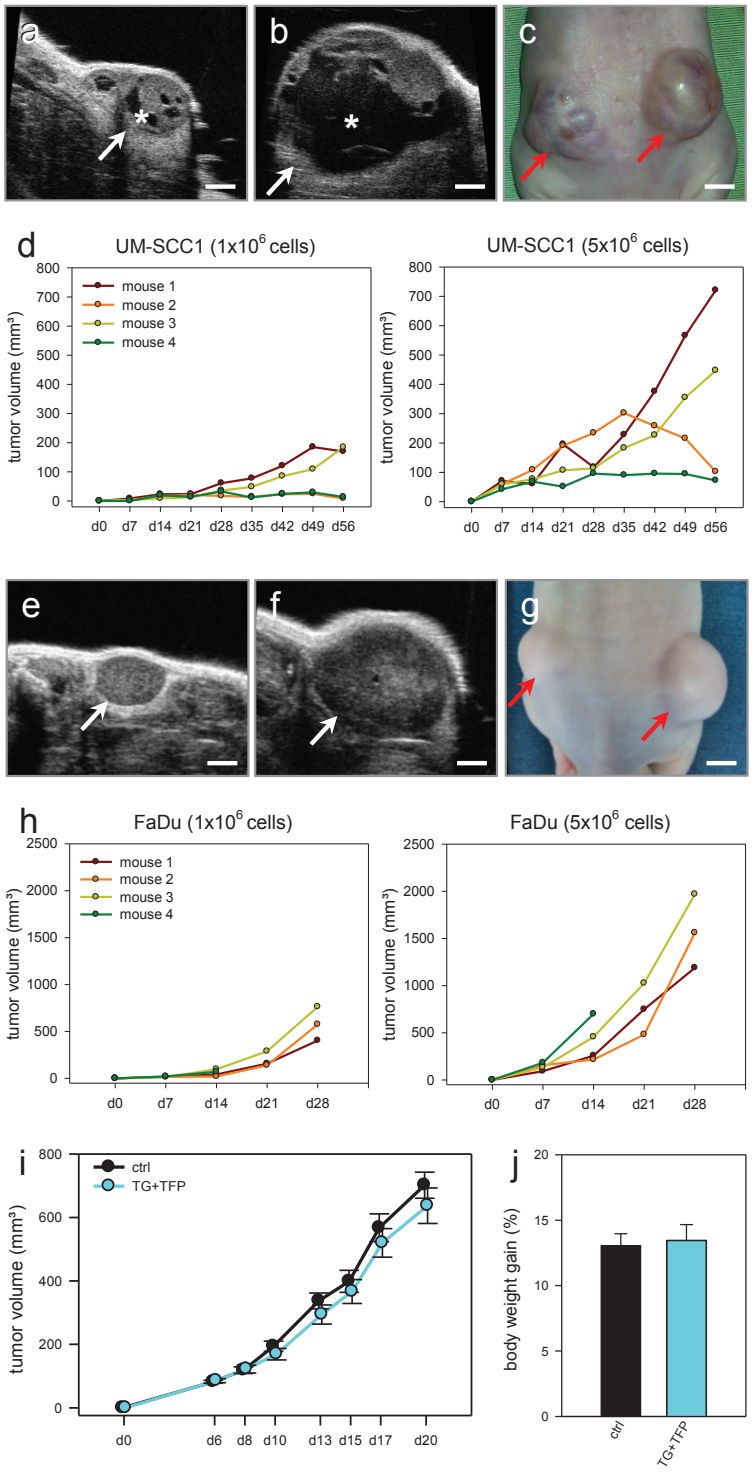

Figure 2: Ultrasound imaging and stereomicroscopic imaging of subcutaneous flank tumors (arrow) after UM-SCC1 (**a-d**) and FaDu (**e-h**) cell inoculation in athymic nude mice. The inoculated cell number for each cell line was 1× 10^6 tumor cells in the left flank (**a,e**) and 5× 10^6 tumor cells in the right flank (**b,f**) of the animals. Note the UM-SCC1 cell tumors developed cysts, which hindered a reliable calculation of the solid tumor mass (asterisk, **a-c**). In contrast the FaDu cell tumors grew faster and showed a solid tumor mass throughout the tumor (**e-g**). **i-j:** Tumor volume measured by caliper three weeks after 1× 10^6 FaDu tumor cells were inoculated in both flanks of 12 vehicle-treated athymic nude mice and 12 athymic nude mice treated with 0.8 mg/kg i.v. Thapsigargin (TG) and 0.5 mg/kg i.p. Trifluoperazine (TFP) three times per week (**i**). The body weight gain of the mice during the observation time is shown at day 20 (**j**). Scale bars: 2 mm (a, b), 4 mm (c), 1.7 mm (e, f), and 5 mm (g).

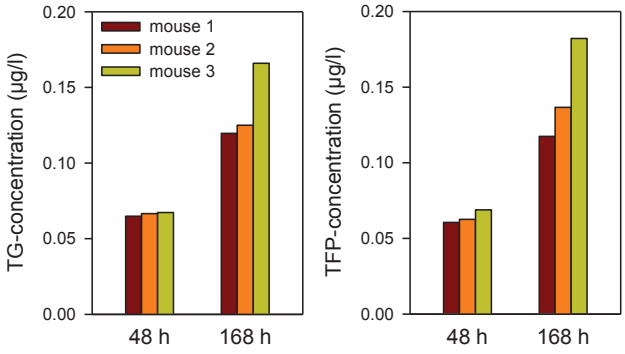

Figure 3: Mass spectrometric measurements of the Thapsigargin (TG)-concentration and Trifluoperazine (TFP)-concentration in serum samples 48 h and 168 h after the treatment of three mice with 1.6 mg/kg i.p. TG and 0.5 mg/kg i.p. TFP at 0 h, 48 h and 96 h.

displayed normal grooming and movement behavior, food and water intake did not differ in-between groups and accelerated respiration rate was not observed. Body weight in the combined-treatment group was significant lower compared to single-treated and vehicle treated groups (Figure 4e).

To monitor the potential effects of the inhibitors on cell proliferation and *SEC62* expression, we evaluated whether Sec62 or Ki67 protein levels were altered by any of our treatments, i.e. performed immunohistochemical staining of the primary tumors. The immunohistochemical detection of proliferating Ki67-positive cells (%) showed an increased proliferation rate in the tumors of vehicle treated mice compared the other treatment groups (Figure 5a-d, j). Interestingly, central necrosis (%) in the tumors

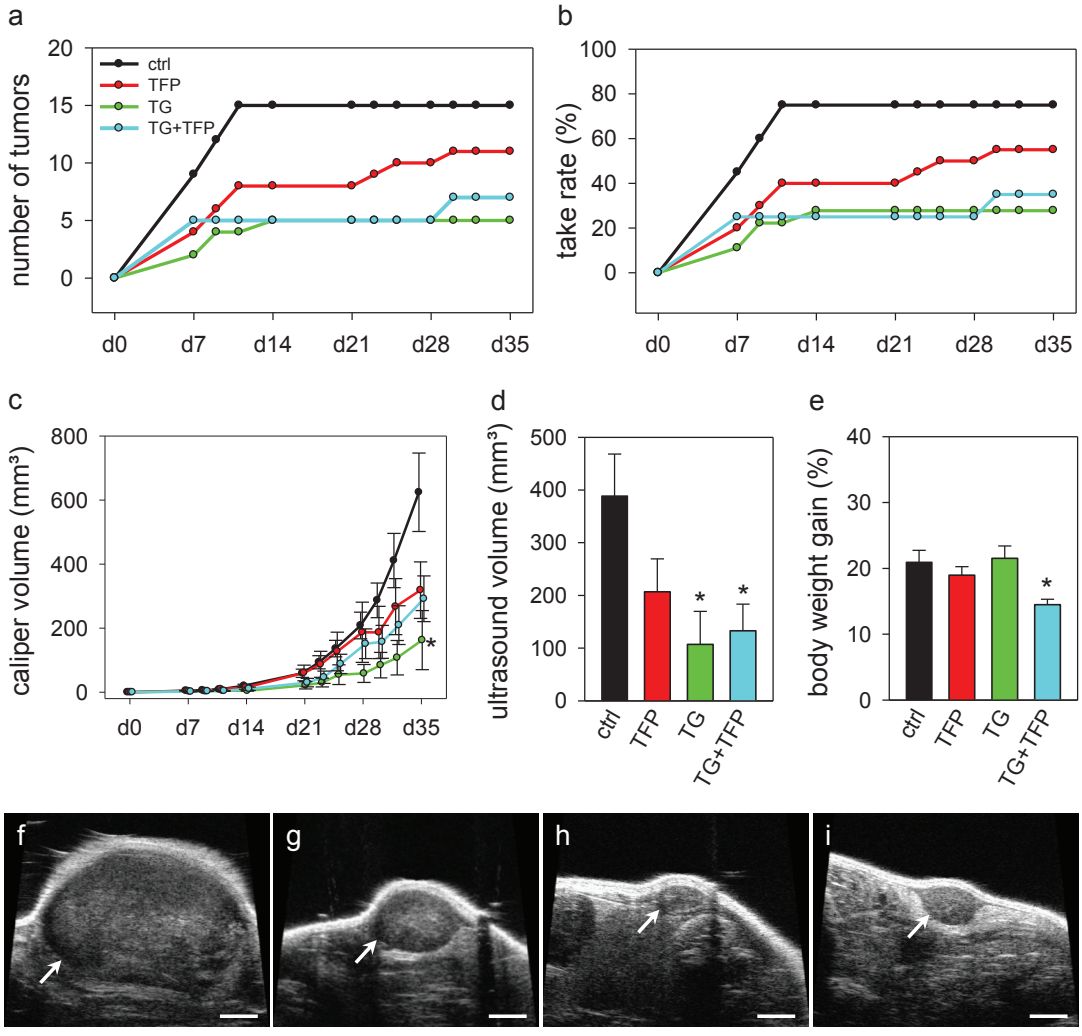

Figure 4: a-b: Number of macroscopic visible FaDu cell tumors and take rate of the tumors in 39 athymic mice treated with the vehicle (ctrl, n=10), 0.5 mg/kg Trifluoperazine (TFP, n=10), 1.6 mg/kg Thapsigargin (TG, n=9) or with both substances (TG+TFP, n=10) three times per week over a time period of 35 days. **c-h:** Caliper measurements (**c**) over the whole observation period and ultrasound measurements (**d,f-i**) on day 35 of the volume of detectable FaDu cell tumors in athymic mice treated with vehicle (**f**), TFP (**g**), TG (**h**) and both substances (**i**). The body weight gain of the mice during the observation time is shown at day 35 (**e**). Scale bars: 2.3 mm. Means ± SEM. *p < 0.05 vs. control.

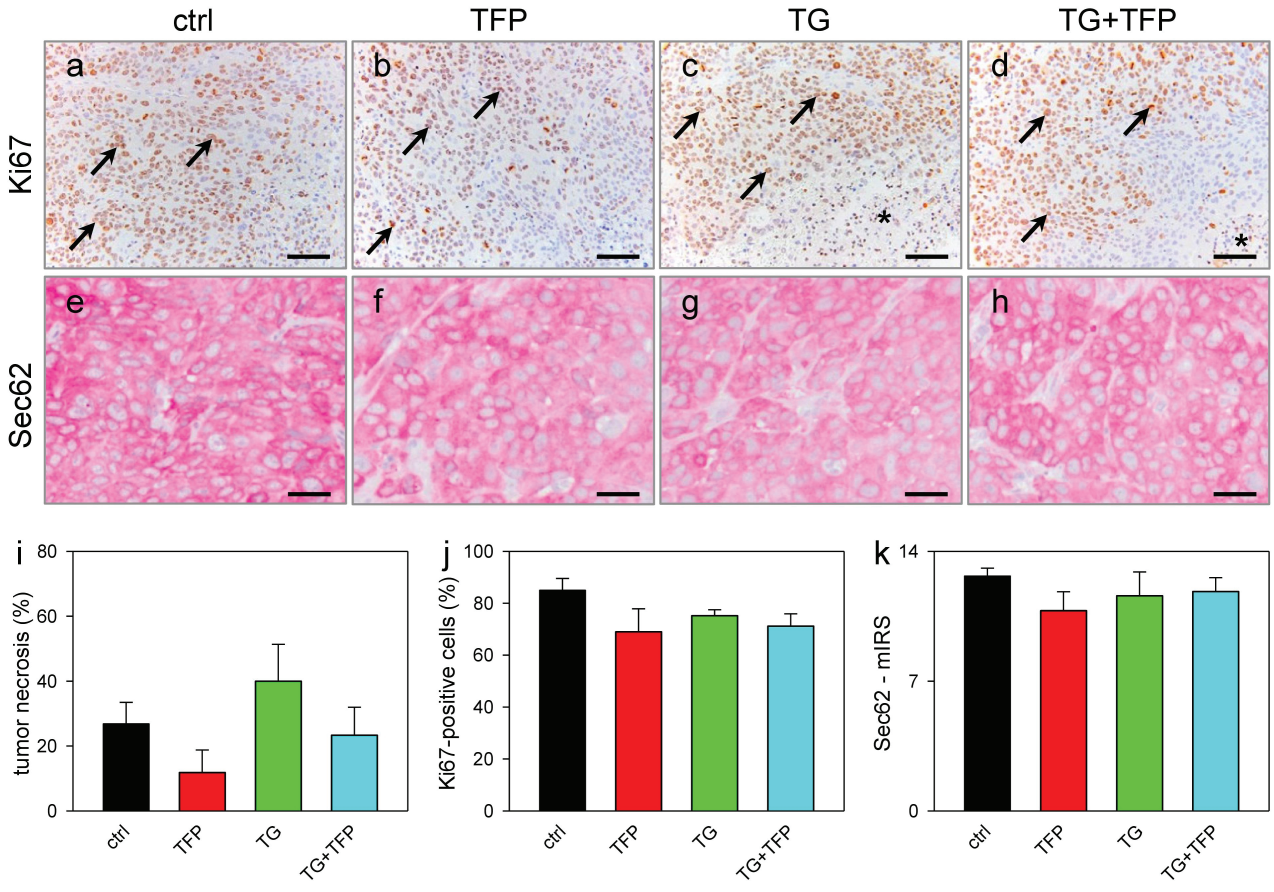

Figure 5: Immunohistochemical stainings of FaDu cell tumors 35 days after inoculation into the flank of athymic mice treated with the vehicle (ctrl, n = 6; **a,e**), 0.5 mg/kg Trifluoperazine (TFP, n = 6; **b,f**), 1.6 mg/kg Thapsigargin (TG, n = 6; **c,g**) or with both substances (TG+TFP, n = 6; **d,h**). The immunohistochemical detection of proliferating Ki67-positive cells (in %, arrows) showed an increased proliferation rate in the tumors of vehicle treated mice compared to the tumors of the other treatment groups (**a-d, j**). Note, that the central necrosis (in %, asterisk) in the tumors was markedly reduced in the Trifluoperazine-treated animals compared to the Thapsigargin-treated animals (**i**). Analyzing the Sec62-mIRS (**e-h, k**), we found slightly reduced staining intensities in the tumors of the treatment groups compared to the tumors of the vehicle-treated group. Scale bars: 80 µm (a-d); 30 µm (e-h). Means ± SEM.

was markedly reduced in the Trifluoperazine-treated animals compared to Thapsigargin-treated (Figure 5i). Furthermore, analysis of the Sec62-mIRS determined a slight decrease in immunoreactivity in the tumors of the treatment groups compared to the vehicle-treated group (Figure 5e-h, k).

Discussion

Cancer treatment with the SERCA-inhibitor Thapsigargin is a promising new approach for a wide variety of cancer entities (2, 3, 6-9). However, our previous studies suggested a higher resistance of *SEC62* over-expressing tumors against this treatment (13, 21-23). As *SEC62* over-expression is a common phenomenon in many cancer entities, an alternative strategy for the treatment of these tumors is needed. *In vitro*, the Calmodulin antagonist Trifluoperazine, which had been in clinical use for schizophrenia treatment, was a promising agent to sensitize tumor cells to Thapsigargin (13, 20). Trifluoperazine binds to Calmodulin thereby impairing its interaction with target molecules. On the molecular level, this leads to increased cytosolic calcium levels and predisposes the cells towards apoptosis. Sec62 acts as a gatekeeper on the Sec61 channel, one of the most important calcium leak channels in the ER membrane. The Trifluoperazine mode of action antagonizes the Sec62-overproduction effect and may pave the way for treatment of these tumors. In this study, we have shown

the impact of Thapsigargin and Trifluoperazine treatment alone and in combination, on heterotopic tumors induced by inoculation of human head and neck squamous cell carcinoma (FaDu) in the mouse flank. The seeding of the tumor cells and/or the growth rate were significantly reduced by these treatments. The effective concentration of the two substances in combination did not induce toxic effects, making the therapeutic use of Trifluoperazine a potential tool for the treatment of patients with Sec62-overproducing tumors. Future work will address the efficiency of the combinatorial therapy in a metastasis model.

Acknowledgements: We are grateful for the technical assistance of Janine Becker (Institute for Clinical & Experimental Surgery, Homburg/Saar). This work was funded by Bundesministerium für Wirtschaft und Energie (SIGNO FKZ 03SHWB051) and the Deutsche Forschungsgemeinschaft (SFB 894).

References

1. Hirsch F.R., Suda K., Wiens J., and Bunn P.A. Jr. New and emerging targeted treatments in advanced non-small-cell lung cancer. Lancet, 2016, 388, 1012-1024.
2. Andersen T.B., Lopez C.Q., Manczak T., Martinez, K., and Simonsen, H.T. Thapsigargin--from Thapsia L. to mipsagargin. Molecules, 2015, 20, 6113-6127.
3. Mahalingam D., Wilding G., Denmeade S., Sarantopoulas J., Cosgrove D., Cetnar J., *et al.* Mipsagargin, a novel thapsigargin-based PSMA-activated prodrug: results of a first-in-man phase I clinical trial in patients with refractory, advanced or metastatic solid tumours. Br. J. Cancer 2016, 114, 986-994.
4. Xu C., Ma H., Inesi G., Al-Shawi M.K., and Toyoshima C. Specific structural requirements for the inhibitory effect of thapsigargin on the Ca2+ ATPase SERCA. J Biol Chem, 2004, 279, 17973-17979.
5. Jakobsen C.M., Denmeade S.R., Isaacs J.T., Gady A., Olsen C.E., and Christensen S.B. Design, synthesis, and pharmacological evaluation of thapsigargin analogues for targeting apoptosis to prostatic cancer cells. Journal of Medicinal Chemistry, 2001, 44, 4696-4703.
6. Andrews S.P., Tait M.M., Ball, M., and Ley, S.V. Design and total synthesis of unnatural analogues of the sub-nanomolar SERCA inhibitor thapsigargin. Org & Biomol Chem, 2007, 5, 1427-1436.
7. Dubois C., Vanden Abeele, F., Sehgal, P., Olesen, C., Junker, S., Christensen, S.B., *et al*. Differential effects of thapsigargin analogues on apoptosis of prostate cancer cells: complex regulation by intracellular calcium. FEBS J, 2013, 280, 5430-5440.
8. Vander Griend D.J., Antony L., Dalrymple S.L., Xu Y., Christensen S.B., Denmeade S.R., and Isaacs J.T. Amino acid containing thapsigargin analogues deplete androgen receptor protein via synthesis inhibition and induce the death of prostate cancer cells. Mol Cancer Ther, 2009, 8, 1340-1349.
9. Denmeade S.R. and Isaacs, J.T. The SERCA pump as a therapeutic target: making a "smart bomb" for prostate cancer. Cancer Biol Ther, 2005, 4, 14-22.
10. Denmeade S.R., Jakobsen C.M., Janssen S., Khan S.R., Garrett E.S., Lilja H., *et al.* Prostate-specific antigen-activated thapsigargin prodrug as targeted therapy for prostate cancer. J Natl Cancer Inst, 2003, 95, 990-1000.
11. Doan N.T., Paulsen E.S., Sehgal P., Moller J.V., Nissen P., Denmeade S.R., *et al.* Targeting thapsigargin towards tumors. Steroids, 2015, 97, 2-7.
12. Wang H.L., Wang S.S., Song W.H., Pan Y., Yu H.P., Si T.G., *et al.* Expression of prostate-specific membrane antigen in lung cancer cells and tumor neovasculature endothelial cells and its clinical significance. PLoS One, 2015, 10, e0125924.
13. Greiner M., Kreutzer B., Lang S., Jung V., Adolpho C., Unteregger G., *et al.* Sec62 protein content is crucial for the ER stress tolerance of prostate cancer. The Prostate, 2011, 71, 1074-1083.
14. Meyer H.A., Grau H., Kraft R., Kostka S., Prehn S., Kalies K.U., and Hartmann E. Mammalian Sec61 is associated with Sec62 and Sec63. J Biol Chem, 2000, 275, 14550-14557.
15. Tyedmers J., Lerner M., Bies C., Dudek J., Skowronek M.H., Haas I.G., *et al.* Homologs of the yeast Sec complex subunits Sec62p and Sec63p are abundant proteins in dog pancreas microsomes. Proc Natl Acad Sci USA, 2000, 97, 7214-7219.
16. Muller L., de Escauriaza M.D., Lajoie P., Theis M., Jung M., Muller A., *et al.* Evolutionary gain of function for the ER membrane protein Sec62 from yeast to humans. Mol Biol Cell, 2010, 21, 691-703.
17. Lang S., Erdmann F., Jung M., Wagner R., Cavalie A., and Zimmermann, R. Sec61 complexes form ubiquitous ER Ca2+ leak channels. Channels (Austin), 2011, 5, 228-235.
18. Erdmann F., Schauble N., Lang S., Jung M., Honigmann A., Ahmad M., *et al.* Interaction of calmodulin with Sec61alpha limits Ca2+ leakage from the endoplasmic reticulum. EMBO J, 2011, 30, 17-31.
19. Harsman A., Kopp A., Wagner R., Zimmermann R., and Jung M. Calmodulin regulation of the calcium-leak channel Sec61 is unique to vertebrates. Channels (Austin) 2011, 5, 293-298.
20. Schauble N., Lang S., Jung M., Cappel S., Schorr S., Ulucan O., *et al.* BiP-mediated closing of the Sec61 channel limits Ca2+ leakage from the ER. EMBO J, 2012, 31, 3282-3296.
21. Linxweiler M., Schorr S., Schauble N., Jung M., Linxweiler J., Langer F., *et al.* Targeting cell migration and the endoplasmic reticulum stress response with calmodulin antagonists: a clinically tested small molecule phenocopy of SEC62 gene silencing in human tumor cells. BMC Cancer, 2013, 13, 574.
22. Greiner M., Kreutzer B., Jung V., Grobholz R., Hasenfus A., Stohr R.F., *et al.* Silencing of the SEC62 gene inhibits migratory and invasive potential of various tumor cells. Int J Cancer, 2011a, 128, 2284-2295.
23. Linxweiler M., Linxweiler J., Barth M., Benedix J., Jung V., Kim Y.J., *et al.* Sec62 bridges the gap from 3q amplification to molecular cell biology in non-small cell lung cancer. Am J Pathol, 2012, 180, 473-483.
24. Wemmert S., Willnecker V., Kulas P., Weber S., Lerner C., Berndt S., *et al.* Identification of CTNNB1 mutations, CTNNB1 amplifications, and an Axin2 splice variant in juvenile angiofibromas. Tumour Biol, 2016, 37, 5539-5549.

25. Tomayko M.M. and Reynolds C.P. Determination of subcutaneous tumor size in athymic (nude) mice. Cancer Chemother Pharmacol, 1989, 24,148-154.
26. Remmele W. and Stegner H.E. Recommendation for uniform definition of an immunreactive score (IRS) for immunohistochemical detection (ER-ICA) in breast cancer tissue. Pathologe 1987, 8, 138-140.
27. Tang L., Shukla P.K., and Wang Z.J. Trifluoperazine, an orally available clinically used drug, disrupts opioid antinociceptive tolerance. Neurosci Lett, 2006, 397, 1-4.